Title

Short: Prediction of fetal blood oxygen content in response to partial occlusion of maternal aorta

Permalink

Authors

Qian, Weitai
Zhong, Hongtao
Ghiasi, Soheil

Publication Date

DOI

Short: Prediction of fetal blood oxygen content in response to partial occlusion of maternal aorta

Weitai Qian[a,*], Hongtao Zhong[a], Soheil Ghiasi[a]

[a]Dept. of Electrical and Computer Engineering, University of California Davis, Davis, CA, 95618, USA

Abstract

Acute hemorrhage in pregnancy may lead to maternal and/or fetal morbidity or mortality. In emergency medicine, blockage of the aorta via an inflatable endovascular balloon, technically referred to Resuscitative Endovascular Balloon Occlusion of the Aorta (REBOA), is used to manage hemorrhage. However, the application of REBOA in pregnancy needs to strike a balance between two competing objectives of limiting maternal blood loss and ensuring fetal wellness, for which one would need to predict the impact of regulated blood pressure on fetal wellness. To address this problem, we propose an efficient machine learning-based method to predict the temporal impact of the distal Mean Arterial Blood Pressure (dMAP) controlled by the REBOA on the oxygen content in the fetal blood. Evaluation of the algorithm on data collected from *in-vivo* experiments from pregnant ewe animal models exhibits mean absolute error of 0.61, 1.09, 1.42, 1.70 mmHg, and coefficient of determination of 0.95, 0.86, 0.76, 0.64 for prediction of partial pressure of oxygen in fetal arterial blood, a key predictor of fetal wellness, in 2.5, 5, 7.5, 10-minute prediction horizons, respectively.

Keywords

Intrapartum hemorrhage; Resuscitative Endovascular Balloon; Occlusion of the Aorta (REBOA); Time-series representation; Fetal assessment; Machine learning; Autoencoder

1. Introduction

Hemorrhage has been the leading cause of maternal mortality in the world Nathan (2019), and is associated with 27% of all maternal deaths James et al. (2022). Intrapartum hemorrhage, which occurs during labor and delivery, may result from various factors, such as placental abruption, placenta previa, vasa previa, and ruptured uterus Hutchon & Martin (2002). Excessive bleeding during labor leads to fetomaternal complications which necessitate prompt intervention. Studies have shown that prevention of hemorrhage will significantly improve maternal outcomes Alexander & Wortman (2013), and a large proportion of trauma-induced death can be prevented Drake et al. (2020). Many studies and clinical trials have shown effective treatments for obstetric hemorrhage, including blood transfusion, surgery, medication, etc. Shevell & Malone (2003); Baird (2017); Trikha &

*Corresponding author: wtqian@ucdavis.edu.

Singh (2018), and Resuscitative Endovascular Balloon Occlusion of the Aorta (REBOA) is one of emerging tools for the management of hemorrhage for obstetricians. This procedure involves placing an inflatable balloon catheter in the patient's aorta to control blood flow. REBOA was typically performed on adult trauma patients Brenner (2015); Morrison et al. (2016); Bulger et al. (2019); Petrone et al. (2019), but many studies have demonstrated its potential in the obstetric and pediatric domains for managing hemorrhage Manzano-Nunez et al. (2018); Barba & Gutierrez (2018); Fernandez & Reed (2020); Campagna et al. (2020); Riazanova et al. (2021).

The usage of REBOA has several advantages over traditional surgical approaches. It is a minimally invasive procedure that can be performed quickly at the patient's bedside, allowing for rapid intervention in a critical situation Stannard et al. (2011); England et al. (2020). It also avoids the need for major surgery, which can be associated with significant risks. Many clinical cases of REBOA usage have been investigated including positive cases Morrison et al. (2016); Sambor (2018); Petrone et al. (2019) and the potential complications Biffl et al. (2015); Uchino et al. (2016); Junior et al. (2018), but the impact of REBOA on fetal health in pregnant subjects is largely unexplored. During pregnancy, the fetus accesses oxygen, and other nutrients, through diffusion processes across the placenta. REBOA regulates placental blood pressure, which in turn impacts fetal blood oxygen content. Therefore, while REBOA can help with the management of maternal hemorrhage, it may also reduce fetal blood oxygen content.

Fig. 1 visualizes the qualitative trade-off between maternal and fetal well-being and distal blood pressure, which is assumed to approximate the maternal blood pressure at the placenta. When the aortic balloon is inflated more, distal blood pressure and maternal hemorrhage are reduced, however, the in-utero fetus may not be able to access a sufficient amount of oxygen, which could lead to adverse neonatal outcomes, such as hypoxic ischemic encephalopathy (HIE). On the other hand, deflating the balloon would increase maternal blood loss, while facilitating fetal access to oxygen (in the short term).

The objective of this paper is to take the first steps towards characterizing the qualitative relationship depicted in Fig. 1. Specifically, we develop a predictive method using which, we predict the temporal impact of REBOA on fP_aO_2, the partial pressure of oxygen in fetal arterial blood, which is a key measure of fetal wellness. The proposed machine learning (ML) based approach is evaluated using empirical data collected in animal studies involving pregnant ewe models in which, REBOA is used to induce controlled fetal hypoxemia. The algorithm is evaluated under different prediction horizons.

2. Study Design

2.1. Hypoxic Lamb Experiment

In this study, we designed and operated hypoxic lamb experiments on the pregnancy sheep model, since sheep models have been repeatedly proven that are applicable to human pregnancy physiology Barry & Anthony (2008); Fong et al. (2020); Vali et al. (2021); Qian et al. (2023). 15 sheep experiments were conducted in the past three years (2020, 2021, and

2022) under the approval of the Institutional Animal Care and Use Committee (IACUC) and included in this study.

In each pregnant sheep experiment (Fig. 2), REBOA was implemented by inserting an endovascular balloon catheter into the ewe's abdominal aorta through the left femoral artery. A femoral artery line was placed near the catheter to monitor the distal Mean Arterial Pressure (dMAP). Two carotid lines were placed on ewe's and fetal necks respectively to collect the blood samples from the mother and baby, and blood samples were used for Arterial Blood Gas (ABG) analysis as the ground truth. The balloon catheter was gradually inflated to control the dMAP during the experiment. A stepwise fashion was operated that dMAP started at 50mmHg and was incrementally reduced by 5mmHg per step (45mmHg, 40mmHg, etc.). Each step was maintained for 10 minutes, and three blood draws were collected at 2.5-, 5- and 10-min for both ewe and baby for ABG tests which monitored the health condition of the ewe and fetus. The hypoxic round would be terminated when two consecutive readings of fetal oxygen saturation ($fSaO_2$) were below 15%. Then the balloon catheter was fully deflated which allowed the fetus to recover for 45 minutes and two blood samples were collected at 30- and 45 -min. The next hypoxic round would be performed if the $fSaO_2$ was above 15%, and three rounds were initially scheduled for each sheep. The time length of each sheep experiment ranges from 2 to 5 hours since the length of each round and the number of rounds differs. In total, we collected around 56 hours of sheep data.

2.2. Dataset Preparation

The data we collected from the sheep experiments included continuous dMAP reading and discrete ABG analysis. dMAP was sampled at 0.2Hz (1 reading for every 5 seconds) and applied a moving median filter to remove outliers during measurement. For the discrete ABG analysis, we performed PCHIP interpolation Rabbath & Corriveau (2019) to 0.2Hz for each ABG parameter to match the dMAP frequency. In this study, we focused on the fetal partial pressure of oxygen (fP_aO_2) as the targeting ABG parameter. It denotes the pressure exerted on the arterial wall by oxygen in a mixture of gases, and it was in the range of [0, 30] for our in-uterus baby lambs. An example of dMAP tracing with interpolated fP_aO_2 from one sheep experiment is shown in Fig. 3. The dMAP was maintained in each step for around 10 min and decreased, and ripples on dMAP imply the hemodynamics in the distal aorta.

The individual sample was then captured by a shifting window (length = l) with 10 seconds overlapping on the time series data, so the time length of each sample is $t = l/0.2$ second. The value of l determined the prediction horizon of fP_aO_2, and different values of l were evaluated. This windowing process was applied to both dMAP and fP_aO_2 time series for all 15 sheep to generate the dataset $\left\{ \sum_{s=1}^{15} P_s, \sum_{s=1}^{15} Q_s \right\}$, where P_s denotes the dMAP data for sheep s and Q_s denotes interpolated fP_aO_2 data for sheep s. They could be represented as:

$$P_s = \sum_{i=1}^{m} P_s^i = \sum_{i=1}^{m} \left(p_{(0)}^i, p_{(1)}^i, p_{(3)}^i, \ldots, p_{(l)}^i \right)_s$$

(1)

$$Q_s = \sum_{i=1}^{m} Q_s^i = \sum_{i=1}^{m} \left(q_{(0)}^i, q_{(1)}^i, q_{(3)}^i, \ldots, q_{(l)}^i \right)_s$$

(2)

where P_s^i is the i-th sample in the sheep s dataset with length l, and m is the number of samples in this sheep's dataset. m is a variable among different sheep depending on the sheep experiment time length. The total number of samples in the dataset is between 19,000 to 20,000 depending on the selection of l.

3. Predictive Model for Fetal Partial Pressure of Oxygen

3.1. Machine Learning Workflow

We proposed an ML pipeline to predict the fP_aO_2 in the near future given the initial fP_aO_2 reading and the temporal dMAP tracing. The workflow is shown in Fig. 4. Two major components consist of this method: the autoencoder for dMAP compression and regressor for fP_aO_2 prediction. Firstly, the dMAP dataset $\sum_{s=1}^{15} P_s$ was normalized so that all data is in the range [0, 1]. Then it was split into training and test set, where one sheep was used as the test set and all other 14 sheep were used for reconstruction training. The dMAP training set was used to train the autoencoder, and then both training and test dMAP samples were compressed to individual vectors for downstream regression, where the vector set was noted as $\sum_{s=1}^{15} Z_s^i$. Therefore, two sets of fixed-length vectors were sent to a regressor: 1) training set contained vectors representing 14 sheep used in autoencoder training; 2) test set contained vectors representing 1 sheep never observed by the autoencoder. Then the regressor learned the function between $\left(Z_s^i, \left(q_{(0)}^i \right)_s \right)$ and $\left(q_{(l)}^i \right)_s$. Test set was used to evaluate this method and test its reliability when the prediction horizon increased. 15-fold cross-validation, where each sheep was used as test set once, was applied to reduce the potential bias caused by the individual difference of subjects. Thus, this ML workflow could be formulated as:

$$Z_s^i = g\left(p_{(0)}^i, p_{(1)}^i, p_{(3)}^i, \ldots, p_{(l)}^i \right)$$

(3)

$$Y_s^i = \left(q_{(l)}^i \right)_s = f\left(Z_s^i, \left(q_{(0)}^i \right)_s \right)$$

(4)

where autoencoder applied function g to find the compressed representation Z_s^i from the i-th dMAP sample in sheep s and l determined the prediction horizon. Regressor could be viewed as the function f to find the relation between the label Y_s^i and $\left(Z_s^i, \left(q_{(0)}^i \right)_s \right)$, where Y_s^i is the final reading of fP_aO_2 in the prediction horizon.

3.2. Autoencoder for dMAP Compression

Autoencoder is an unsupervised method that learns compressed codings of unlabeled data Baldi (2011), and it has the advantage of reducing noise of the input. An autoencoder was proposed to learn the compressed representation of the time-series dMAP input. It had two major components encoder and decoder, and the training and test set for the autoencoder were the same, where, in this case, $\sum P_s$ (14 sheep) was used for autoencoder training in each trial of cross-validation.

Fig. 5 showed our architecture of autoencoder. An input dMAP sample with length l was fed into two consecutive convolutional layers that each followed with a pooling layer to reduce the dimension of the feature maps. The output of this encoder was a compressed vector with length 8. As for the decoder part, a similar structure was designed to recreate the input. Upsampling was applied to recover the dimension of the original time-series, and two convolutional layers were added to project the features to the output. The training of the autoencoder uses Mean Squared Error (MSE) as the loss function.

3.3. Regression

With the trained autoencoder, we were able to extract the compressed codes for each input in both the training and test set. These codes combined with initial fP_aO_2 reading $\left(q_{(0)}^i\right)_s$ were then used as the input of a regressor to fit the resulting $\left(q_{(l)}^i\right)_s$. Different regressors were compared and also evaluated with various prediction horizons. Here are the regressors we tested: (1) Linear Regressor (LR). (2) Light Gradient Boosting Machine (LGBM). (3) Extreme Gradient Boosting (XGB). (4) Kernel Ridge Regressor (KRR). (5) CatBoost Regressor (CBR). (6) Elastic Net (EN). (7) Bayesian Ridge Regressor (BRR). (8) Gradient Boosting (GB). (9) Support Vector Regressor (SVR).

Regressors were trained with the training set containing 14 sheep and then evaluated with the test set. The performance of the model was assessed by two metrics Mean Absolute Error (MAE) and coefficient of determination r-squared $\left(r^2\right)$ between prediction values and true labels.

4. Results

4.1. Autoencoder for dMAP Reconstruction

The autoencoder was trained with 14 sheep data where the input had different time horizons {2.5, 5, 7.5, 10} min. Fig. 6 shows some examples of dMAP reconstruction when the input time length is 5-min. The red curve denotes the original dMAP signal and the blue curve is the reconstructed signal. The blue curve has fewer ripples but keeps the trend of the red curve, which means some noise has been canceled and the main features are maintained. The usage of an autoencoder allows the downstream steps to be more efficient since a long time-series is compressed and represented as a vector with size 8. But it needs to be mentioned that, as the input signal is longer, the MSE of the autoencoder training is higher.

4.2. fP_aO_2 Regression with Variable Prediction Horizon

Cross-validation with 15 folds was used to evaluate the proposed method. Fig. 7 shows the MAE and r^2 of linear regressor when each sheep was used as test set, and the last column shows the average. The average MAE are {0.62, 1.09, 1.42, 1.70} in mmHg for prediction horizon {2.5min, 5min, 7.5min, 10min}, and the average r^2 are {0.95, 0.86, 0.76, 0.64} respectively. For each sheep, the MAE increases when the prediction horizon increases. The reason could be that a fixed-length vector was used to represent the dMAP signal. As the dMAP length increased, the information was more compressed, meaning that vector length 8 might not be sufficient to represent the dMAP time-series. This thought was confirmed by the increasing MSE error of the autoencoder while longer time-series was sent for training. The coefficient of determination $\left(r^2\right)$, on the other hand, shows the proportion of variation in the dependent variable could be explained by the independent variable decreasing with the prediction horizon increased. That said, the correlation between $\left(Z_s^i, (q_{(0)}^i)_s\right)$ and $(q_{(t)}^i)_s$ is lower when the time interval is higher.

Different regressors were evaluated to find the relation between final fP_aO_2 and initial fP_aO_2 given the dMAP tracing between two timestamps. Table 1 shows the performance where two metrics are considered: 1)MAE assesses how close the predicted final fP_aO_2 with ground truth fP_aO_2; 2)r^2 assesses how much variation the predicted final fP_aO_2 can be explained by the input. Therefore, a lower MAE with higher r^2 is more desirable. LR and BRR give the lowest MAE and highest r^2 among all regressors for prediction horizon = {5min, 7.5min, 10min} and KRR is the best for 2.5min. But the performance of all regressors with 2.5-min prediction horizon is close. Therefore, overall the linear regressor and bayesian ridge regressor outperform other regressors in terms of both error and correlation.

5. Conclusion

In this study, we proposed a pipeline to predict fP_aO_2, a critical fetal ABG parameter, given a short history of dMAP with the initial reading of this parameter. We showed the feasibility of compressing dMAP tracing and using regression models to predict fP_aO_2 in near future. The results gave the average MAE = {0.61, 1.09, 1.42, 1.70} and r^2 = {0.95, 0.86, 0.76, 0.64} for different prediction horizon {2.5min, 5min, 7.5min, 10min} after cross validation among 15 sheep. We also concluded that the compressed representation of dMAP given initial fP_aO_2 is likely to have a linear correlation with final fP_aO_2 in a near future. This method could help doctors to prospect the impact of dMAP control on the baby and provide information on immediate REBOA regulation, which potentially improves the well-being of both mother and baby. Our future work will focus on improving prediction accuracy with long prediction horizons, and integrating information from external measurements, such as maternal heart rate and fetal heart rate, to improve the robustness and reliability of obstetric REBOA procedure.

Acknowledgments

References

Alexander JM, & Wortman AC (2013). Intrapartum hemorrhage. Obstet Gynecol Clin North Am, 40, 15–26. [PubMed: 23466133]

Baird EJ (2017). Identification and management of obstetric hemorrhage. Anesthesiology Clinics, 35, 15–34. doi 10.1016/J.ANCLIN.2016.09.004 [PubMed: 28131117]

Baldi P (2011). Autoencoders, unsupervised learning and deep architectures. In Proceedings of the 2011 International Conference on Unsupervised and Transfer Learning Workshop -Volume 27 UTLW'11 (p. 37–50). JMLR.org.

Barba NL, & Gutierrez K (2018). Use of a resuscitative, endovascular balloon occlusion of the aorta (reboa) device to save the life of a jehovah witness patient with placenta percreta. Journal of Obstetric, Gynecologic Neonatal Nursing, 47, S62. URL: http://www.jognn.org/article/S0884217518301862/fulltexthttp://www.jognn.org/article/S0884217518301862/abstracthttps://www.jognn.org/article/S0884-2175(18)30186-2/abstract. doi 10.1016/j.jogn.2018.04.121

Barry J, & Anthony R (2008). The pregnant sheep as a model for human pregnancy. Theriogenology, 69, 55–67. doi 10.1016/j.theriogenology.2007.09.021 [PubMed: 17976713]

Biffl WL, Fox CJ, & Moore EE (2015). The role of reboa in the control of exsanguinating torso hemorrhage. Journal of Trauma and Acute Care Surgery, 78, 1054–1058. URL: https://journals.lww.com/jtrauma/Fulltext/2015/05000/The_role_of_REBOA_in_the_control_of_exsanguinating.24.aspx. doi 10.1097/TA.000000000000609 [PubMed: 25909430]

Brenner M (2015). Reboa and catheter-based technology in trauma. Journal of Trauma and Acute Care Surgery, 79, 174–175. URL: https://journals.1ww.com/jtrauma/Fulltext/2015/07000/REBOA_and_catheter_based_technology_in_trauma.25.aspx. doi 10.1097/TA.0000000000000701 [PubMed: 26091331]

Bulger EM, Perina DG, Qasim Z, Beldowicz B, Brenner M, Guyette F, Rowe D, Kang CS, Gurney J, Dubose J, Joseph B, Lyon R, Kaups K, Friedman VE, Eastridge B, & Stewart R (2019). Clinical use of resuscitative endovascular balloon occlusion of the aorta (reboa) in civilian trauma systems in the usa, 2019: a joint statement from the american college of surgeons committee on trauma, the american college of emergency physicians, the national association of emergency medical services physicians and the national association of emergency medical technicians. Trauma Surgery Acute Care Open, 4, 376. URL: /pmc/articles/PMC6802990//pmc/articles/PMC6802990/?report=abstracthttps://www.ncbi.nlm.nih.gov/pmc/articles/PMC6802990/ doi 10.1136/TSAC0-2019-000376

Campagna GA, Cunningham ME, Hernandez JA, Chau A, Vogel AM, & Naik-Mathuria BJ (2020). The utility and promise of resuscitative endovascular balloon occlusion of the aorta (reboa) in the pediatric population: An evidence-based review reboa in pediatric patients. Journal of Pediatric Surgery, 55, 2128–2133. URL: http://www.jpedsurg.org/article/S0022346820300956/fulltexthttp://www.jpedsurg.org/article/S0022346820300956/abstracthttps://www.jpedsurg.org/article/S0022-3468(20)30095-6/abstract. doi 10.1016/j.jpedsurg.2020.01.052 [PubMed: 32061369]

Drake SA, Holcomb JB, Yang Y, Thetford C, Myers L, Brock M, Wolf DA, Persse D, Naik-Mathuria BJ, Wade CE, & Harting MT (2020). Establishing a regional pediatric trauma preventable/potentially preventable death rate. Pediatr Surg Int, 36, 179–189. [PubMed: 31701301]

England EC, Spear CR, Huang DD, Weinberg J, Bogert JN, Gillespie T, & Mankin J (2020). Reboa as a rescue strategy for catastrophic vascular injury during robotic surgery. Journal of Robotic Surgery, 14, 473–477. URL: https://link.springer.com/article/10.1007/s11701-019-01011-3. doi 10.1007/S11701-019-01011-3/TABLES/1 [PubMed: 31463880]

Fernandez AG, & Reed MJ (2020). Obstetric hemorrhage. Evidence-Based Critical Care, (pp. 759–765). URL: https://link.springer.com/chapter/10.1007/978-3-030-26710-0_101. doi 10.1007/978-3-030-26710-0_101.

Fong DD, Yamashiro KJ, Johnson MA, Vali K, Galganski LA, Pivetti CD, Farmer DL, Hedriana HL, & Ghiasi S (2020). Validation of a novel transabdominal fetal oximeter in a hypoxic fetal lamb model. Reproductive Sciences, 27, 1960–1966. URL: https://link.springer.com/article/10.1007/s43032-020-00215-5. doi 10.1007/S43032-020-00215-5/FIGURES/4 [PubMed: 32542541]

Hutchon SP, & Martin WL (2002). Intrapartum and postpartum bleeding. Current Obstetrics Gynaecology, 12, 250–255. doi 10.1054/CUOG.2002.0271

James AH, Federspiel JJ, & Ahmadzia HK (2022). Disparities in obstetric hemorrhage outcomes. Res Pract Thromb Haemost, 6, e12656. [PubMed: 35146237]

Junior MAR, Feng CY, Nguyen AT, Rodrigues VC, Bechara GE, de Moura RR, & Brenner M (2018). The complications associated with resuscitative endovascular balloon occlusion of the aorta (reboa). World Journal of Emergency Surgery, 13, 1–6. URL: https://link.springer.com/articles/10.1186/s13017-018-0181-6https://link.springer.com/article/10.1186/s13017-018-0181-6. doi 10.1186/S13017-018-0181-6/FIGURES/1 [PubMed: 29371878]

Manzano-Nunez R, Escobar-Vidarte MF, Naranjo MP, Rodriguez F, Ferrada P, Casallas JD, & Ordoñez CA (2018). Expanding the field of acute care surgery: a systematic review of the use of resuscitative endovascular balloon occlusion of the aorta (reboa) in cases of morbidly adherent placenta. European Journal of Trauma and Emergency Surgery, 44, 519–526. URL: https://link.springer.com/article/10.1007/s00068-017-0840-4. doi 10.1007/S00068-017-0840-4/FIGURES/3 [PubMed: 28929283]

Morrison JJ, Galgon RE, Jansen JO, Cannon JW, Rasmussen TE, & Eliason JL (2016). A systematic review of the use of resuscitative endovascular balloon occlusion of the aorta in the management of hemorrhagic shock. Journal of Trauma and Acute Care Surgery, 80, 324–334. URL: https://journals.lww.com/jtrauma/Fulltext/2016/02000/A_systematic_review_of_the_use_of_resuscitative.22.aspx. doi 10.1097/TA.0000000000000913 [PubMed: 26816219]

Nathan LM (2019). An overview of obstetric hemorrhage. Seminars in Perinatology, 43, 2–4. doi 10.1053/J.SEMPERI.2018.11.001 [PubMed: 30691692]

Petrone P, Pérez-Jiménez A, Rodríguez-Perdomo M, Brathwaite CEM, & Joseph DK (2019). Resuscitative Endovascular Balloon Occlusion of the Aorta (REBOA) in the Management of Trauma Patients: A Systematic Literature Review. Am Surg, 85, 654–662. [PubMed: 31267908]

Qian W, Vali K, Kasap B, Pivetti CD, Theodorou CM, Kulubya ES, Yamashiro KJ, Wang A, Hedriana HL, Farmer DL, & Ghiasi S (2023). Continuous transabdominal fetal pulse oximetry (tfo) in pregnant ewe models under induced fetal hypoxia. American Journal of Obstetrics Gynecology, 228, S242–S243. URL: http://www.ajog.org/article/S0002937822013254/fulltexthttp://www.ajog.org/article/S0002937822013254/abstracthttps://www.ajog.org/article/S0002-9378(22)01325-4/abstract. doi 10.1016/J.AJOG.2022.11.441

Rabbath C, & Corriveau D (2019). A comparison of piecewise cubic hermite interpolating polynomials, cubic splines and piecewise linear functions for the approximation of projectile aerodynamics. Defence Technology, 15, 741–757.

Riazanova OV, Reva VA, Fox KA, Romanova LA, Kulemin ES, Riazanov AD, & Ioscovich A (2021). Open versus endovascular reboa control of blood loss during cesarean delivery in the placenta accreta spectrum: A single-center retrospective case control study. European Journal of Obstetrics Gynecology and Reproductive Biology, 258, 23–28. doi 10.1016/J.EJOGRB.2020.12.022 [PubMed: 33388487]

Sambor M (2018). Resuscitative Endovascular Balloon Occlusion of the Aorta for Hemorrhage Control in Trauma Patients: An Evidence-Based Review. J Trauma Nurs, 25,33–37. [PubMed: 29319648]

Shevell T, & Malone FD (2003). Management of obstetric hemorrhage. Seminars in Perinatology, 27, 86–104. doi 10.1053/SPER.2003.50006 [PubMed: 12641305]

Stannard A, Eliason JL, & Rasmussen TE (2011). Resuscitative endovascular balloon occlusion of the aorta (reboa) as an adjunct for hemorrhagic shock. Journal of Trauma -

Injury, Infection and Critical Care, 71, 1869–1872. URL: https://journals.lww.com/jtrauma/Fulltext/2011/12000/Resuscitative_Endovascular_Balloon_Occlusion_of.62.aspx. doi 10.1097/TA.0B013E31823FE90C.

Trikha A, & Singh PM (2018). Management of major obstetric haemorrhage. Indian Journal of Anaesthesia, 62, 698. URL: /pmc/articles/PMC6144554//pmc/articles/PMC6144554/?report=abstracthttps://www.ncbi.nlm.nih.gov/pmc/articles/PMC6144554/. doi 10.4103/IJA.IJA_448_18 [PubMed: 30237595]

Uchino H, Tamura N, Echigoya R, Ikegami T, & Fukuoka T (2016). "reboa" - is it really safe? a case with massive intracranial hemorrhage possibly due to endovascular balloon occlusion of the aorta (reboa). The American Journal of Case Reports, 17, 810. URL: http://www.jognn.org/article/S0884217518301862/fulltexthttp://www.jognn.org/article/S0884217518301862/abstracthttps://www.jognn.org/article/S0884-2175(18)30186-2/abstract. doi 10.12659/AJCR.900267 [PubMed: 27799653]

Vali K, Kasap B, Qian W, Theodorou CM, Lihe T, Fong DD, Pivetti CD, Kulubya ES, Yamashiro KJ, Wang A, Johnson MA, Hedriana HL, Farmer DL, & Ghiasi S (2021). Non-invasive transabdominal assessment of in-utero fetal oxygen saturation in a hypoxic lamb model. American Journal of Obstetrics and Gynecology, 224, S604. URL: http://www.ajog.org/article/S0002937820323759/fulltexthttp://www.ajog.org/article/S0002937820323759/abstracthttps://www.ajog.org/article/S0002-9378(20)32375-9/abstract. doi 10.1016/j.ajog.2020.12.999
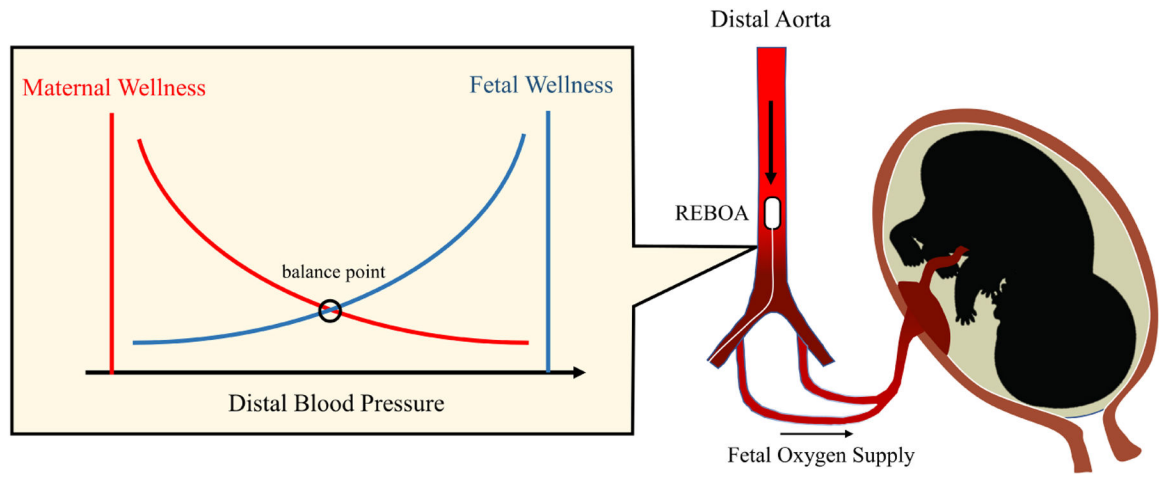
Fig. 1.
The wellness of mother and baby have an inverse response, in the short term, to the distal blood pressure with respect to the REBOA.
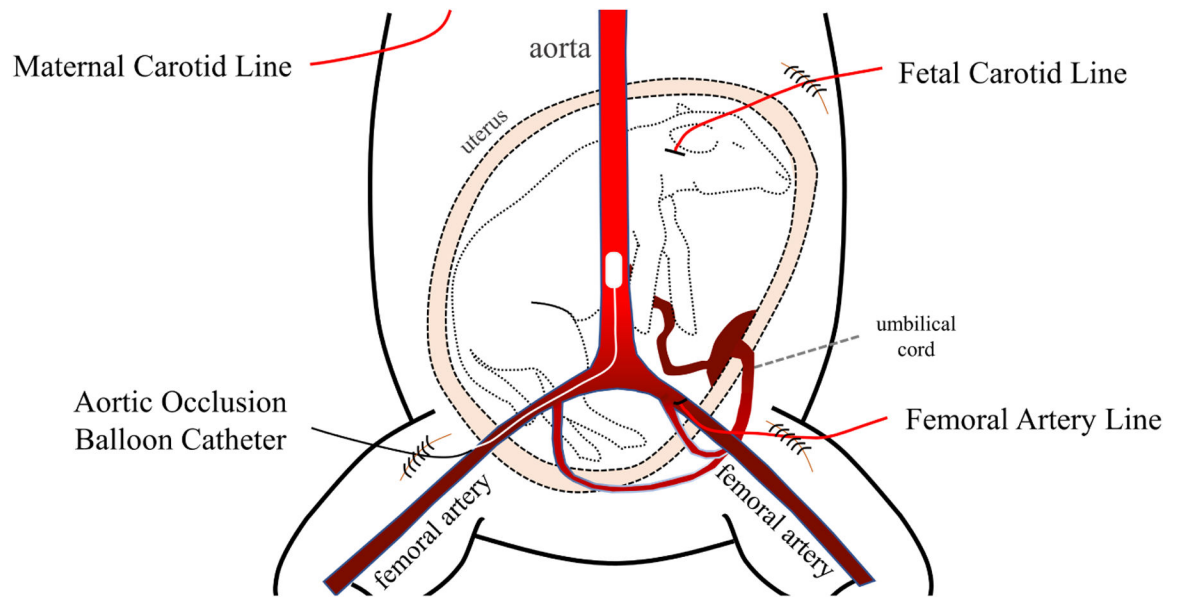
Fig. 2.
Sketch of the animal experiment: hypoxic lamb in pregnant ewe model (Vessels are simplified and brought to top for demonstration). REBOA is placed through the left femoral artery and blood pressure is monitored on the right femoral artery. Fetal and maternal carotid lines are placed for blood draws.
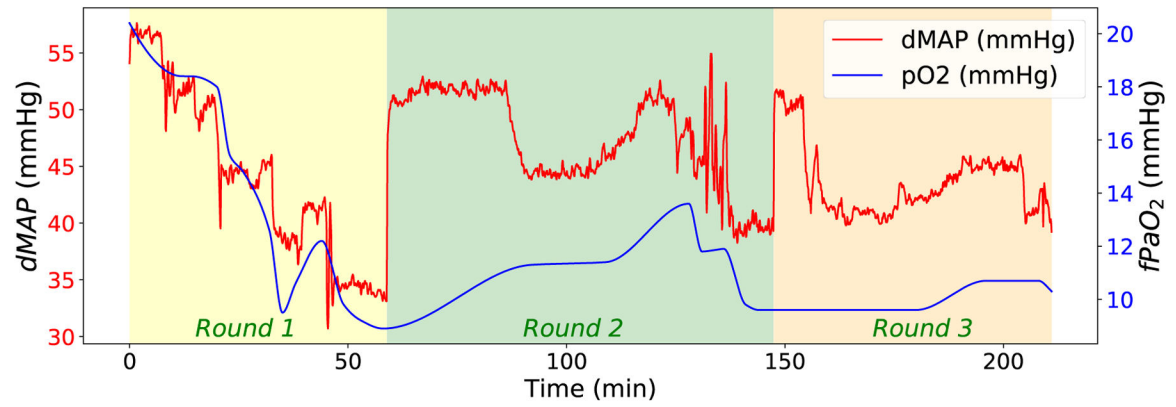
Fig. 3.

A demonstration of dMAP recording and one interpolated fetal ABG parameter (fP_aO_2) from one sheep experiment. This sheep experiment consists of three rounds and it lasts about 3.5 hours. Background colors differ for each round.
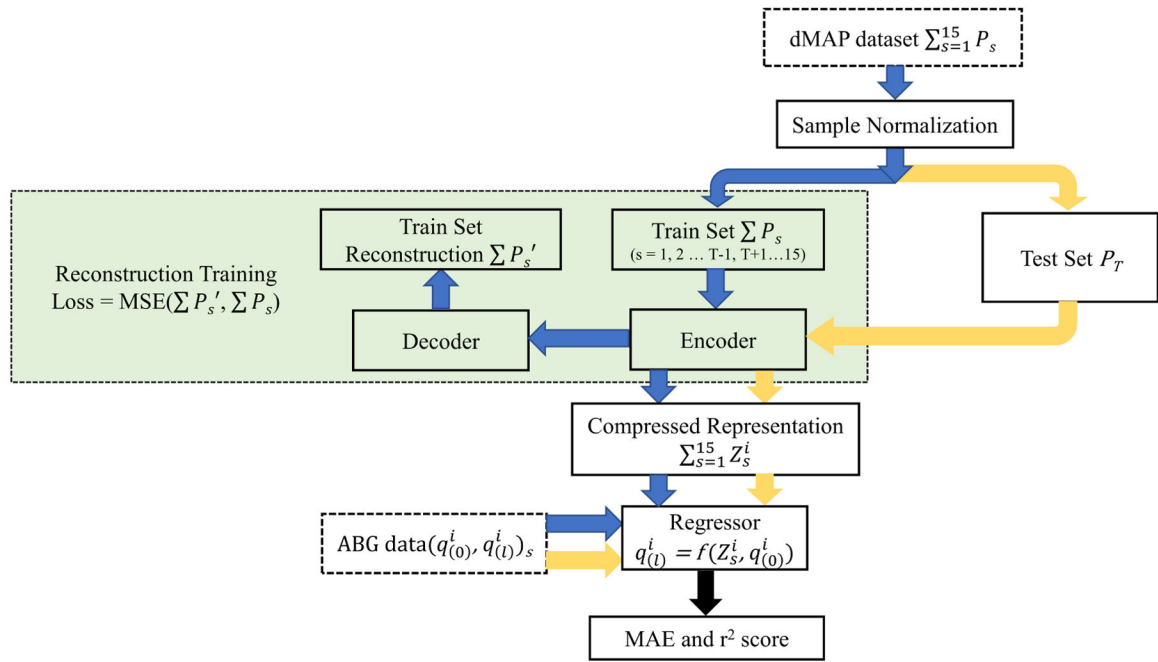
Fig. 4.

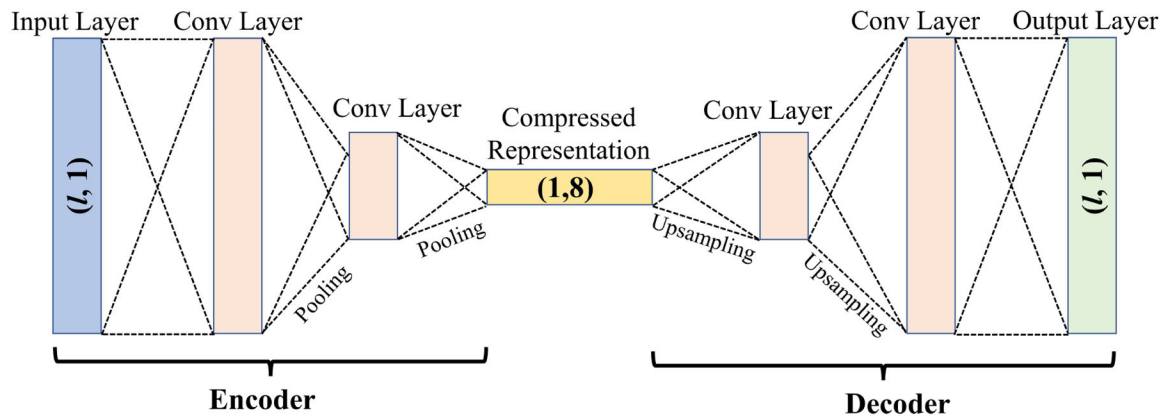A proposed workflow based on time-series autoencoder to predict ABG parameter in near future

Fig. 5.
A convolutional autoencoder to reconstruct the dMAP signal. The encoder took a $(l, 1)$ time-series sequence was compressed to a $(1, 8)$ feature vector, and the decoder tried to recover the input.
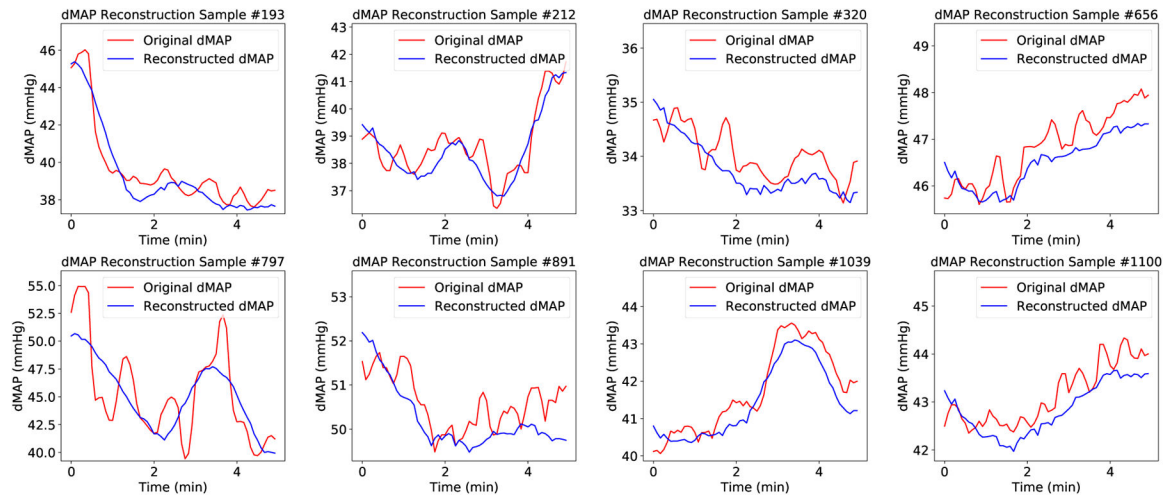
Fig. 6.
Eight selected samples for dMAP reconstruction. In each subplot, y-axis is the dMAP
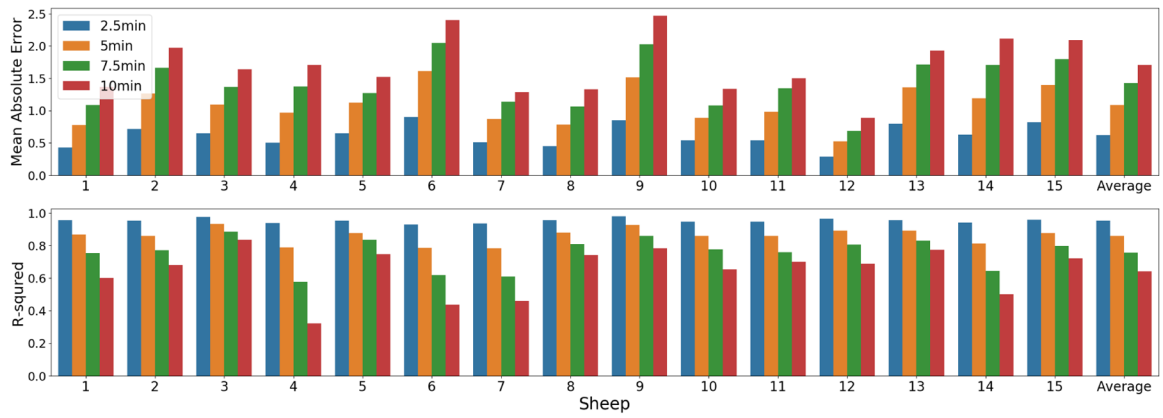(mmHg), and x-axis is the time length.

Fig. 7.

The MAE and coefficient of determination results of linear regression for all 15 sheep.
Each column denotes the error when this certain sheep was used as the test set. Four colors
represent the MAE/r^2 values when different prediction horizons were evaluated.

Table 1.

Different regressors were used to fit the relation between compressed dMAP history and final fP_aO_2 prediction given the initial fP_aO_2 reading. The best performance in each row is highlighted in bold.

Regressor	LR		LGBM		XGB		KRR		CBR		EN		BRR		GB		SVR	
Metric	mae	r^2	mae	r^2	mae	r^2	mae	r^2	mae	r^2	mae	r^2	mae	r^2	mae	r^2	mae	r^2
2.5min	0.62	**0.95**	0.70	**0.95**	0.75	0.94	**0.61**	**0.95**	0.73	0.94	0.67	**0.95**	0.62	**0.95**	0.66	**0.95**	0.63	**0.95**
5min	**1.09**	**0.86**	1.29	0.81	1.37	0.79	1.11	0.85	1.30	0.80	1.22	0.83	**1.09**	**0.86**	1.21	0.83	1.14	0.85
7.5min	**1.42**	**0.76**	1.74	0.64	1.86	0.57	1.47	0.74	1.75	0.63	1.69	0.68	**1.42**	**0.76**	1.62	0.68	1.58	0.71
10min	**1.70**	**0.64**	2.08	0.46	2.20	0.39	1.73	0.63	2.11	0.42	2.10	0.51	**1.70**	**0.64**	2.04	0.49	1.83	0.61